Image of an emitting dipole by a superlens

Tran Minh Hien and Ho Trung Dung

Institute of Physics, Academy of Sciences and Technology, 1 Mac Dinh Chi Street, District 1, Ho Chi Minh City, Vietnam

(Received 10 August 2011; revised manuscript received 22 November 2011; published 11 January 2012)

We consider the emission pattern of a three-dimensional pointlike dipole situated near a left-handed-medium slab. Unlike earlier work, we focus on the direction normal to the slab surface. It is shown that the evanescent field may help to narrow the major peak of the image created by the propagating field. We point out that care has to be taken when applying Snell's law to the superlens problem. In particular, it cannot explain why the focus is shifted away from the ideal position when material absorption decreases below some threshold value.

DOI: 10.1103/PhysRevA.85.015804 PACS number(s): 42.25.Bs, 42.79.Bh, 42.30.Wb, 42.50.Nn

I. INTRODUCTION

Negative index materials were first discussed by Veselago [1], who showed that simultaneous negative dielectric permittivity ε and magnetic permeability μ imply a negative index of refraction. In these materials, the electric field, the magnetic field, and the wave vector of a plane wave form a left-handed system, hence the name left-handed material (LHM). The refraction of a beam at a vacuum-medium interface is governed by Snell's law,

$$\sin\theta_t = \frac{1}{n}\sin\theta_i, \tag{1}$$

where n is the medium refractive index and θ_i is the incidence angle measured with respect to a line normal to the interface. When loss due to medium absorption is negligible, n can be treated as a real quantity and θ_t bears the meaning of the beam exit angle. In common materials, the refractive index n is positive and a deflected beam exits to the opposite side of the surface normal. Left-handed materials, by contrast, have a negative n and would deflect the exiting beam to the same side of the surface normal. This phenomenon was experimentally observed [2].

For a single slab in free space, applying Eq. (1) twice to the two vacuum-medium interfaces, one finds that the slab produces a focusing effect [1]. What is even more interesting is that a slab of LHM can enhance the evanescent nonpropagating components of radiation that are usually confined to the immediate vicinity of a source. This led to the suggestion that the entire information of a source can be restored in the image, giving rise to the possibility of a perfect lens whose image resolution can beat the traditional diffraction limit of a wavelength [3]. The proposal for a perfect lens provoked heated debates [4,5], particularly due to the divergence of the field in between the slab and the focus point. To deal with this mathematical difficulty, schemes where extra charges are placed at the foci have been proposed [6] and realistic factors such as the inherent material loss have been taken into account [7–10]. Based on the wave-vector cutoff of the transmitted spectrum, it has been shown that the subwavelength performance of a LHM-based flat lens is limited to the near-field zone [7,10]. Related problems such as the spontaneous decay of a pointlike dipole emitter placed in the slab's vicinity [11] and the diffusion of the focal points from the standpoint of Snell's law [12] were discussed.

Since the wave-vector cutoff used in Refs. [7,10] is with respect to the component of the wave vector parallel to the surface, the derived resolution limit is valid in the plane of the surface only. Here we explore the possibility of the superlensing effect in the direction normal to the surface of the LHM slab via a consideration of the emission pattern of a point dipole located in its vicinity. Unlike Refs. [7,10], we employ a method based on the numerics. Namely, the emission pattern is first calculated using propagating waves alone (strictly speaking only the intensity of the total field is measurable), then is compared with that produced by the total field. We find that the inclusion of the evanescent field indeed gives rise to some narrowing of the major peak of the image. Furthermore, we show that while many features of the imaging system can be explained by the real version of Snell's law, it cannot predict the exact positions of the foci.

II. NUMERICAL RESULTS

Being excited by some suitable means, a dipole emitter (position $\mathbf{r}_A$, transition frequency ω_A, dipole moment $\mathbf{d}_A$) undergoes the process of spontaneous decay and emits light. Proceeding along the same lines as in the case of pure dielectrics [13] and using properties of the Green tensor [14], the electromagnetic field intensity $I(\mathbf{r},t)$ can be found to be

$$I(\mathbf{r},t) \simeq |\mathbf{F}(\mathbf{r},\mathbf{r}_A,\omega_A)|^2 e^{-\Gamma t}, \tag{2}$$

where, after dropping a small quantum correction,

$$\mathbf{F}(\mathbf{r},\mathbf{r}_A,\omega_A) \simeq -\frac{ik_A^2}{\varepsilon_0}\boldsymbol{G}(\mathbf{r},\mathbf{r}_A,\omega_A)\mathbf{d}_\mathrm{A}. \tag{3}$$

Here $\Gamma = (2k_A^2/\hbar\varepsilon_0)\,\mathbf{d}_\mathrm{A}\mathrm{Im}\,\boldsymbol{G}(\mathbf{r}_A,\mathbf{r}_A,\omega_A)\mathbf{d}_\mathrm{A}$ is the dipole spontaneous decay rate with $k_A = \omega_A/c$, and $\boldsymbol{G}(\mathbf{r},\mathbf{r}',\omega)$ is the Green tensor that describes the media surrounding the dipole. Equation (2) together with Eq. (3) generalize the results of [13] to the case of an arbitrary dispersing and absorbing magnetodielectrics. Apart from a time-dependent exponentially decaying factor, the spatial pattern of emission is determined by $|\mathbf{F}(\mathbf{r},\mathbf{r}_A,\omega_A)|^2$.

Let z be the direction normal to the structure surface, the dipole be located in layer 0, the slab occupy layer 1, and the field point be located in layer 2. The Green tensor can be expanded into plane waves

$$\boldsymbol{G}^{(20)}(\mathbf{r},\mathbf{r}_\mathrm{A},\omega) = \frac{i}{4\pi}\int_0^\infty dk_\parallel k_\parallel \frac{e^{i\beta_0 z_\mathrm{A}+i\beta_2 z}}{2\beta_2}\,\tilde{\boldsymbol{G}}^{(20)}(\mathbf{r},\mathbf{r}_\mathrm{A},\omega,k_\parallel), \tag{4}$$

where $\mathbf{k}_\parallel = k_x\hat{x} + k_y\hat{y}$ and $\beta_j = \sqrt{\varepsilon_j(\omega)\mu_j(\omega)\frac{\omega^2}{c^2} - k_\parallel^2}$, $j = 0,1,2$, and the specific form of $\tilde{\boldsymbol{G}}^{(20)}$ can be found in Ref. [15]. Next, we assume that the slab is placed in vacuum, $\varepsilon_{0,2} = \mu_{0,2} = 1$, its permittivity and permeability being close to -1 and having small, positive imaginary parts which characterize the degree of material absorption $\epsilon_1 = \mu_1 = -1 + i\gamma$, $\gamma \ll 1$. Note that $\gamma \sim 10^{-1}$ is the typical range of absorption in presently realized LHMs. The Green tensor can be decomposed into two parts,

$$\boldsymbol{G}^{(20)}(\mathbf{r},\mathbf{r}_\mathrm{A},\omega_A) = (\boldsymbol{G}^{(20)})_1 + (\boldsymbol{G}^{(20)})_2, \tag{5}$$

where $(\boldsymbol{G}^{(20)})_1 = \int_0^{k_A} dk_\parallel \cdots$ represents propagating waves and $(\boldsymbol{G}^{(20)})_2 = \int_{k_A}^{\infty} dk_\parallel \cdots$ represents evanescent waves.

A. Ten-wavelength thick slab

The emission pattern along the z axis for some representative values of γ is plotted in Fig. 1 using Eqs. (3) and (4). The position of the image, and the half width at half maximum (HWHM) of the total field peak and that of the propagating field peak are listed in Table I. Consider first the case of an atomic transition dipole moment oriented parallel to the slab surface. If we compare the HWHM of the peaks due to the propagating field, $(\delta I)_{x1}/\lambda_A$ listed in Table I, with that in the lossless case $(\delta I)_{x1}/\lambda_A \simeq 0.443$, it is evident that material loss broadens the peaks. The broadening decreases with a decreasing γ. For $\gamma \sim 10^{-5}$ and below, the broadening is insignificant. Now if we compare the width of the peak associated with the propagating field (Table I, line 4) with that of the total field (Table I, line 3), we find that the latter is narrower than the first for $\gamma = 10^{-5}, 10^{-7}, 10^{-9}$ (boldface).

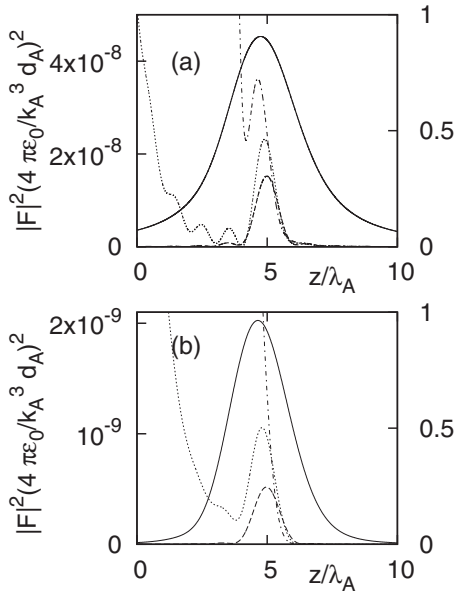

FIG. 1. The emission pattern along the z axis as a function of the distance from the (1/2) interface to the field point. The parameters are $z_A = 5\lambda_A$, $d = 10\lambda_A$, and $\epsilon_1 = \mu_1 = -1 + i\gamma$ with $\gamma = 10^{-1}$ (solid line), 10^{-3} (dashed line), 10^{-5} (dotted line), and 10^{-12} (dot-dashed line). For the first case the scale is to the left of the figure, while for the last three cases the scale is to the right. The dipole moment is (a) parallel and (b) normal to the slab surface.

TABLE I. Position and HWHM of the image. $x_0(z_0)$,$(\delta I)_x[(\delta I)_z]$, and $(\delta I)_{x1}[(\delta I)_{z1}]$ are the image position, the HWHM of the total peak, and the HWHM of the peak associated with the propagating field for $x(z)$-oriented dipole moment.

γ	10^{-1}	10^{-3}	10^{-5}	10^{-7}	10^{-9}
x_0/λ_A	4.747	4.987	4.897	4.824	4.754
$(\delta I)_x/\lambda_A$	1.685	0.49	**0.441**	**0.437**	**0.436**
$(\delta I)_{x1}/\lambda_A$	1.674	0.489	**0.445**	**0.443**	**0.443**
z_0/λ_A	4.643	4.974	4.801	—	—
$(\delta I)_z/\lambda_A$	1.326	0.566	0.547	—	—
$(\delta I)_{z1}/\lambda_A$	1.321	0.564	0.532	—	—

It can be seen from Fig. 1(a) that for large material loss ($\gamma = 10^{-1}$ and 10^{-3}, solid and dashed curves), the evanescent field is mostly absorbed by the slab, whereas for small material loss ($\gamma = 10^{-5}$ and 10^{-12}, dotted and dot-dashed curves), its enhancement is clearly evident. The peak narrowing thus can be attributed to the contribution from the evanescent field. Numerical results in the table show that when γ is reduced from 10^{-7} to 10^{-9}, the resolution is not improved as much as when it is reduced from 10^{-5} to 10^{-7}. The same trend has been noticed with respect to the resolution in the x direction [7,10]. As γ is reduced even further, the enhancement of the evanescent field by the slab is so strong that the image is submerged in the evanescent field tail [Fig. 1(a), dot-dashed curve]. The general picture is more and more resembling that in the case of zero absorption where the evanescent field between the slab and the focal point diverges.

Let us have a closer look at the peaks' positions. At $\gamma = 10^{-1}$, the curve is peaked away from the ideal focal point $z/\lambda_A = 5$, at a position closer to the surface. When γ decreases from 10^{-1} to 10^{-3}, the peak location approaches the ideal focal point. Since in this range of γ, no evanescent field enhancement is observed [see Fig. 1(a), solid and dashed curves], the shift is due solely to the influence of the material loss on the propagating field. As γ is reduced further from 10^{-3} to 10^{-5}, 10^{-7}, and 10^{-9}, instead of keeping on approaching the ideal focal point, the peak is pulled back toward the slab. The evanescent field, which is enhanced noticeably in this range of γ, obviously causes this reversal in the direction of the shift of the image.

From the above analysis, it becomes clear that there is only a finite range of γ where the peak narrowing can occur. The value of γ must not be too large such that evanescent waves are not completely absorbed by the slab and can contribute to the image. On the other hand, it must not be too small such that the enhanced evanescent waves tail does not swallow up the peak produced by propagating waves. For the parameters used in Fig. 1 and Table I, such an optimal range of γ apparently does not exist for a z-oriented dipole moment [Fig. 1(b)]. This can be explained by the fact that a z-oriented dipole couples more strongly to the evanescent field than an x-oriented dipole does, resulting in that the enhanced evanescent field swallows up the peak before any narrowing can occur.

B. Single-wavelength thick slab

Let us consider now a one-wavelength thick slab. In the case of an x-oriented atomic dipole moment and $\gamma = 10^{-1}$

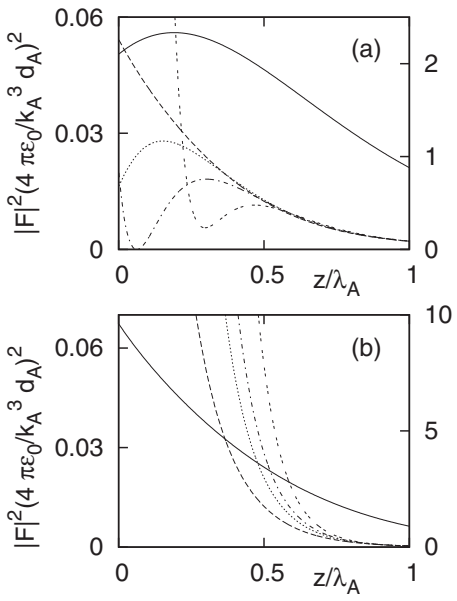

FIG. 2. The emission pattern along the z axis as a function of the distance from the (1/2) interface to the field point. The parameters are $z_A = 0.5\lambda_A$, $d = \lambda_A$, and $\epsilon_1 = \mu_1 = -1 + i\gamma$ with $\gamma = 10^{-1}$ (solid line), 3×10^{-3} (dashed line), 10^{-3} (dotted line), 5×10^{-4} (dot-dashed line), and 10^{-4} (double dashed line). For the first case the scale is to the left of the figure while for the last four cases the scale is to the right. The dipole moment is (a) parallel and (b) normal to the slab surface.

[Fig. 2(a), solid curve], numerical results for evanescent and propagating field separately (not shown) indicate that the first is insignificant in comparison with the latter. The closeness to the surface and the spread of the peak led to the fact that only half of it is visible. For γ in the range from 10^{-1} to 10^{-3}, the peak associated with the propagating field is located close to the surface, at a distance where the propagating and the evanescent fields are comparable. These two interfere destructively, destroying the peak [Fig. 2(a), dashed curve]. As γ is reduced from 10^{-3} (dotted curve) to 10^{-4} (double dashed curve), the peak created by the propagating field is sufficiently far from the surface so that the same trend as in the case of $d = 10\lambda_A$ can take place, that is, the peak gets narrower while its position is shifted toward the ideal focal point at $z = 0.5\lambda_A$. The amount of narrowing achievable here is much more impressive compared to the case of the 10-wavelength thick slab discussed above. Namely, for $\gamma = 10^{-3}$, 5×10^{-4}, and 10^{-4}, the HWHM $(\delta I)_x/\lambda_A$ are 0.25, 0.225, and 0.214, respectively, which are much smaller than the HWHM of the peaks generated by the propagating field alone $(\delta I)_{x1}/\lambda_A =$ 0.452, 0.448, and 0.445. The numbers mean about 50% narrowing. However, there is a tradeoff in that the peaks are strongly asymmetric, that is, the image is distorted. The half peak on the slab side is narrower than that on the other side. This confirms the role of the evanescent field in the peak narrowing because the evanescent field is stronger on the slab side of the peak rather than on the free space side. When γ is decreased further, the growing contribution of the evanescent field gradually swallows up the image peak. This takes place at a larger value of γ than in the case of thicker slabs [cf. Fig. 1] due to a closer proximity of the image to the surface. For slabs thinner than about $0.7\lambda_A$, no clear formation of the image is found. In the case of a z-oriented dipole moment, this already occurs at $d = \lambda_A$, as can be seen from Fig. 2(b).

III. SNELL's LAW

Certain features of the imaging system obtained from the numerical computations above can be inferred from Snell's law. For a complex n, θ_t in Eq. (1) is also complex and no longer has the meaning of an angle of refraction. If we denote by θ_t' the angle between the normal of the surface of constant real phase and the normal of the boundary, then [16]

$$\sin\theta_t' = \frac{1}{N}\sin\theta_i, \tag{6}$$

where

$$N = \sqrt{\sin^2\theta_i + \bar{n}^2 q^2(\cos\gamma - \kappa\sin\gamma)^2}, \tag{7}$$

$$n = \sqrt{\varepsilon_1\mu_1} = \bar{n}(1 + i\kappa), \tag{8}$$

$$q^2\cos 2\gamma = 1 - \frac{1-\kappa^2}{\bar{n}^2(1+\kappa^2)^2}\sin^2\theta_i, \tag{9}$$

$$q^2\sin 2\gamma = \frac{2\kappa}{\bar{n}^2(1+\kappa^2)^2}\sin^2\theta_i. \tag{10}$$

In Eq. (8), $\bar{n}$ and κ are real. For $\varepsilon_1 = \mu_1 = -1 + i\gamma$, we have $\bar{n} = -1$ and $\kappa = -\gamma$.

Equation (6) has the form of Snell's law, but with N depending not only on the refractive index, but also on the incidence angle θ_i. This leads to a degeneration of the focal point into a diffused focal spot [12]. Using the assumption $\gamma \ll 1$ to expand N in terms of κ and keeping only the leading order term, we obtain

$$\sin\theta_t' \simeq \frac{1}{\bar{n}\sqrt{1 + \gamma^2\tan^2\theta_i}}\sin\theta_i. \tag{11}$$

Equation (11) shows that the angle of refraction θ_t' is smaller than that occurring in the absorptionless case. Since the angle of refraction in the medium 2 is equal to θ_i (the configuration under consideration is symmetric), this brings the second focal point closer to the surface, as can be figured out from Fig. 3 after a little geometry. According to Eq. (11), the image always moves toward the ideal focal point as the absorption decreases. The real version of Snell's law thus cannot explain the reversed shift of the image away from the ideal focal point after the material absorption decreases below some threshold value.

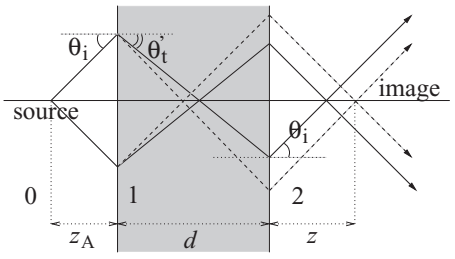

FIG. 3. The shifting and smearing of the image due to material absorption in accordance with the real version of Snell's law. The dashed lines represent rays of light when the material absorption is neglected.

This is because the ray-optics picture represented by Eqs. (6)–(11) does not take into account evanescent waves.

IV. CONCLUSIONS

We have derived a formula for the spatial pattern of the field emitted by a dipole surrounded by an arbitrary magnetodielectrics and used it to investigate the emission pattern of a dipole located near an LHM slab, concentrating on the possibility of the superlensing effect in the direction normal to the surface. The main peak in the image generated by the propagating field alone is compared with that generated by the total field, and a narrowing of the latter is regarded as a signature of the superlensing effect. Some peak narrowing has been found to exist but is very fragile. It manifests itself for slab thicknesses of about a single wavelength only, and at the price of strong image distortion. It favors the dipole orientation parallel to the surface, and is highly sensitive to material absorption. The material absorption must not be too large such that the evanescent field is sufficiently enhanced to contribute to the peak, but not too small such that the tail of the enhanced evanescent field does not swallow up the peak. These limitations are quite severe and may render the superlensing effect impractical. We have shown that due to the contribution of the evanescent waves, the position of the peak shifts in a peculiar way as the material absorption decreases: it first approaches the ideal focal point, then moves away from it. The latter cannot be described by the real version of Snell's law.

ACKNOWLEDGMENTS

This research was supported by NAFOSTED under Grant No. 103.99-2010.03. H.T.D. acknowledges support from the Abdus Salam ICTP.

[1] V. G. Veselago, Sov. Phys. Usp. **10**, 509 (1968).
[2] D. R. Smith, W. J. Padilla, D.C. Vier, S. C. Nemat-Nasser, S. Schultz Phys. Rev. Lett. **84**, 4184 (2000); C. G. Parazzoli, R. B. Greegor, K. Li, B. E. C. Koltenbah, M. Tanielian, *ibid.* **90**, 107401 (2003); G. Dolling, M. Wegener, C. M. Soukoulis, and S. Linden, Opt. Lett. **32**, 53 (2007); H. J. Lezec, J. A. Dionne, and H. A. Atwater, Science **316**, 430 (2007).
[3] J. B. Pendry, Phys. Rev. Lett. **85**, 3966 (2000).
[4] N. Garcia and M. Nieto-Vesperinas, Phys. Rev. Lett. **88**, 207403 (2002).
[5] A. L. Pokrovsky and A. L. Efros, Physica B **338**, 333 (2003).
[6] V. V. Klimov, J. Exp. Theor. Phys. Lett. **89**, 229 (2009); V. V. Klimov, J. Baudon, and M. Ducloy, Europhys. Lett. **94**, 20006 (2011).
[7] L. Shen and S. He, Phys. Lett. A **309**, 298 (2003).
[8] Z. Ye, Phys. Rev. B **67**, 193106 (2003).
[9] R. Merlin, Appl. Phys. Lett. **84**, 1290 (2004).
[10] V. A. Podolskiy and E. E. Narimanov, Opt. Lett. **30**, 75 (2005).
[11] J. Kästel and M. Fleischhauer, Phys. Rev. A **71**, 011804(R) (2005); Q. Cheng and T. J. Cui, Phys. Lett. A **345**, 439 (2005); J.-P. Xu, N.-H. Liu, and S.-Y. Zhu, Phys. Rev. E **73**, 016604 (2006); A. Sambale, D.-G. Welsch, Ho Trung Dung, and S. Y. Buhmann, Phys. Rev. A **79**, 022903 (2009); J.-P. Xu, Y.-P. Yang, Q. Lin, and S.-Y. Zhu, *ibid.* **79**, 043812 (2009).
[12] C. Carloz and T. Itoh, *Metamaterials: Transmission Line Theory and Microwave Approximation* (Wiley-Interscience, New York, 2006).
[13] Ho Trung Dung, L. Knöll, and D.-G. Welsch, Phys. Rev. A **64**, 013804 (2001).
[14] Ho Trung Dung *et al.*, Phys. Rev. A **68**, 043816 (2003).
[15] M. S. Tomaš, Phys. Rev. A **51**, 2545 (1995).
[16] M. Born and E. Wolf, *Principles of Optics* (Cambridge University Press, Cambridge, 1999).